Gene Duplication Is an Evolutionary Mechanism for Expanding Spectral Diversity in the Long-Wavelength Photopigments of Butterflies

Francesca D. Frentiu, Gary D. Bernard,† Marilou P. Sison-Mangus,* Andrew Van Zandt Brower,‡ and Adriana D. Briscoe**

*Department of Ecology and Evolutionary Biology, University of California, Irvine; †Department of Electrical Engineering, University of Washington; and ‡Department of Biology, Middle Tennessee State University

Butterfly long-wavelength (L) photopigments are interesting for comparative studies of adaptive evolution because of the tremendous phenotypic variation that exists in their wavelength of peak absorbance (λ_{max} value). Here we present a comprehensive survey of L photopigment variation by measuring λ_{max} in 12 nymphalid and 1 riodinid species using epi-microspectrophotometry. Together with previous data, we find that L photopigment λ_{max} varies from 510–565 nm in 22 nymphalids, with an even broader 505- to 600-nm range in riodinids. We then surveyed the L opsin genes for which λ_{max} values are available as well as from related taxa and found 2 instances of L opsin gene duplication within nymphalids, in *Hermeuptychia hermes* and *Amathusia phidippus*, and 1 instance within riodinids, in the metalmark butterfly *Apodemia mormo*. Using maximum parsimony and maximum likelihood ancestral state reconstructions to map the evolution of spectral shifts within the L photopigments of nymphalids, we estimate the ancestral pigment had a λ_{max} = 540 nm ± 10 nm standard error and that blueshifts in wavelength have occurred at least 4 times within the family. We used ancestral state reconstructions to investigate the importance of several amino acid substitutions (Ile17Met, Ala64Ser, Asn70Ser, and Ser137Ala) previously shown to have evolved under positive selection that are correlated with blue spectral shifts. These reconstructions suggest that the Ala64Ser substitution has indeed occurred along the newly identified blueshifted L photopigment lineages. Substitutions at the other 3 sites may also be involved in the functional diversification of L photopigments. Our data strongly suggest that there are limits to the evolution of L photopigment spectral shifts among species with only one L opsin gene and that opsin gene duplication broadens the potential range of λ_{max} values.

Introduction

Butterfly color vision, like that of other insects, is based on 3 major classes of photoreceptors, with peak sensitivity (λ_{max}) in the ultraviolet (UV, 300–400 nm), blue (B, 400–500), and long-wavelength (L, 500–600) regions of the light spectrum (reviewed in Briscoe and Chittka 2001; Stavenga and Arikawa 2006). At the molecular level, these photopigments are comprised of a retinal-based chromophore (e.g., 11-*cis*-3-hydroxyretinal) surrounded by an opsin protein. The spectral tuning of the photopigment λ_{max} value is achieved through the interaction of the chromophore with critical amino acid residues within the opsin, a mechanism that has been most extensively studied in vertebrate photopigments (Asenjo et al. 1994; Fasick and Robinson 1998; Yokoyama and Radlwimmer 1998; Wilkie et al. 2000). Changes in the polarity of amino acids in the chromophore-binding pocket of opsins, for instance, affect the distribution of electrons in the π-electron system of the chromophore, producing a diversity of λ_{max} values (Honig et al. 1976). In the case of the insect photopigments, the 3 major spectral classes are encoded by ancient duplications, which produced distinct UV, B, and L opsin genes.

Diversification of butterfly photopigments has also occurred through more recent lineage-specific gene duplications. For example, duplicate blue opsins have diversified into blue- and violet-absorbing photopigments in the Pieridae (Arikawa et al. 2005) and duplicate blue opsins have diversified into blue- and blue-green–absorbing photopigments in the Lycaenidae (Sison-Mangus et al. 2006). The extent to which spectral diversification has occurred via natural selection on a single opsin locus, however, is less clear.

To investigate the role of opsin gene duplication versus selection on a single opsin locus in producing spectral diversity, we focused on the L photopigments of butterflies. Earlier photochemical studies suggested some butterfly eyes contain 2 L photopigments, whereas others contain only 1 (Bernard 1979). In the adult compound eye, the papilionid *Papilio xuthus* has 3 L photopigments (λ_{max} = 515 nm, 530 nm, and 575 nm; Arikawa et al. 2003), whereas the pierid *Pieris rapae*, the lycaenid *Lycaena rubidus*, and the nymphalid *Vanessa cardui* each have only one L photopigment (λ_{max} = 563 nm, 568 nm, and 530 nm, respectively; Bernard 1983a; Bernard and Remington 1991; Wakakuwa et al. 2004). Of these families, we selected nymphalids for study because photochemical, molecular, and anatomical work has indicated that the typical nymphalid eye contains only one L photopigment (along with UV and blue photopigments mentioned above) (Briscoe et al. 2003; Sauman et al. 2005; Zaccardi et al. 2006) (see below) and physiological diversity of this photopigment in nymphalids ranges from 510–545 nm (Stavenga 1975; Bernard 1983b; Briscoe and Bernard 2005; Vanhoutte and Stavenga 2005; Frentiu et al. 2007).

Recently, we reported that the 31-nm range of L photopigment variation found within the nymphalid genus *Limenitis* is due to positive selection-driven adaptation at a single L opsin gene (Frentiu et al. 2007). In that analysis, we identified substitutions at 4 amino acid sites (Ile17Met, Ala64Ser, Asn70Ser, and Ser137Ala), which are strongly correlated with blueshifts in L photopigment λmax. We therefore sought to investigate the extent to which substitutions at these sites are correlated with blue spectral shifts in a taxonomically expanded data set of L opsin photopigments.

Key words: visual pigment, gene duplication, Nymphalidae, Riodinidae, opsin, color vision.

E-mail: abriscoe@uci.edu.

Mol. Biol. Evol. 24(9):2016–2028. 2007
doi:10.1093/molbev/msm132
Advance Access publication July 3, 2007

To address this question, we determined the peak absorbance of L photopigments from 12 species of nymphalids and compared them with our previous studies of the L photopigments of 9 other nymphalids performed on the same experimental apparatus. We then examined L opsin transcripts from 8 of the 12 taxa as well as an expanded set of 11 nymphalid species for which no physiological data are available. We included the riodinid *Apodemia mormo* in our screen for L opsin transcripts because its eye contains an unusually redshifted L photopigment (λ_{max} = 600 nm) as well as a second L photopigment (λ_{max} = 505 nm) whose absorbance spectra we report below (Bernard 1979; Bernard et al. 1988). We discovered 3 novel L opsin gene duplications and further evidence that substitutions at the afore mentioned 4 amino acid sites are indeed involved in the evolution of L photopigment spectral shifts. Taken together, our data suggest that gene duplication is an evolutionary mechanism for expanding the spectral diversity of L photopigments in butterflies.

Materials and Methods

Photochemical and Physiological Measurements

Absorption spectra of L photopigment can be measured directly from eyes of completely intact butterflies, thanks to 2 unusual properties. The first is that photoisomerization of the dark-adapted L photopigment (rhodopsin) creates a blueshifted photoproduct (i.e., metarhodopsin) that is unstable (the metarhodopsin photopigment decays more rapidly than the rhodopsin photopigment regenerates). The second unusual property, in many species of butterfly, is that each ommatidium contains a multilayered tracheolar tapetum that creates eyeshine.

Each retinular cell has a rhabdomere, the microvillar membrane of which is packed with photopigment molecules. The 9 rhabdomeres of an ommatidium are fused into a single cylindrical rhabdom that functions as a fiber-optic waveguide. Eyeshine is created by light entering the cornea, traveling down the rhabdom waveguide, reaching the end of the rhabdom, reflecting from the tapetum, and then traveling back out of the eye where it is observable as eyeshine. Because the volume of the rhabdom is packed with photopigment, the reflectance spectrum of eyeshine is influenced by absorption spectra of all photopigments and their photoproducts contained within the volume of the rhabdom.

As described in the supplementary materials and methods (Supplementary Material online), we use an epimicrospectrophotometer to create partial bleaches of L photopigment, measure eyeshine reflectance spectra and difference spectra, and analyze those spectra to estimate the absorption spectrum of L photopigment and its wavelength for maximal absorbance, λ_{max}. We used this method to survey the diversity of L photopigment absorbance spectra in 22 species from 7 nymphalid subfamilies (*Asterocampa leilia*, *Archaeoprepona demophon*, *Danaus plexippus*, *Heliconius charithonia*, *Heliconius erato*, *Heliconius hecale*, *Agraulis vanillae*, *Anartia jatrophae*, *Euphydryas chalcedona*, *Hermeuptychia hermes*, *Limenitis archippus archippus*, *Limenitis archippus floridensis*, *Limenitis arthemis astyanax*, *Limenitis lorquini*, *Limenitis weidemeyerii*, *Inachis io*, *Junonia coenia*, *Nymphalis antiopa*, *Neominois ridingsii*, *Oeneis chryxus*, *Siproeta stelenes*, and *V. cardui*; table 1).

We also present the absorbance spectra of the R505 and R600 photopigments of the riodinid *A. mormo* including details not found in earlier reports (Bernard 1979; Bernard et al. 1988). Estimates of absorbance spectra for *H. erato* R555 and *A. mormo* R505 were based on optophysiological measurements of spectral sensitivity. Details are provided in the supplementary materials and methods (Supplementary Material online).

Butterfly Tissue Sampling

We then sampled the L opsin gene from 9 of the 13 taxa for which we were able to measure L photopigment λ_{max} values and combined these with previously published L opsin sequences for *H. erato* and *Heliconius sara* (Hsu et al. 2001; Zaccardi et al. 2006), and *D. plexippus* (Sauman et al. 2005). The L opsin genes of the riodinid butterfly, *A. mormo*, are of special interest taxonomically because this represents an exemplar of the only other butterfly family (out of 5) not yet examined for opsin genes, and this family together with the lycaenids are sister taxon to the nymphalids (Campbell et al. 2000). In addition, we sampled 11 other nymphalid taxa for which no physiological data are available. Butterflies were either caught by the authors as adults in the field (table 1) or kindly provided as pupae or adults by Carol Boggs (*H. charithonia*), John Emmel (*A. mormo*), Matthew Garhart (*N. ridingsii*), Antonia Monteiro (*Bicyclus anynana*), and Lincoln Brower (*D. plexippus*). Tissue was preserved for either RNA or genomic DNA extraction.

Polymerase Chain Reaction, Cloning, and Sequencing

Total mRNA was extracted from 8 species (*A. vanillae*, *Speyeria mormonia*, *E. chalcedona*, *B. anynana*, *Coenonympha tullia*, *O. chryxus*, *N. ridingsii*, and *A. mormo*) using TRIzol (Invitrogen, Carlsbad, CA). Double-stranded complementary DNA (cDNA) was synthesized from total RNA using the Marathon cDNA Amplification Kit (BD Biosciences Clontech, Mountain View, CA). The 3′-RACE (rapid amplification of cDNA ends) products were amplified with a degenerate primer (5′-GAA CAR GCW AAR AAR ATG A-3′) by polymerase chain reaction (PCR) (2 min at 94 °C; 35 cycles of 30 s at 94 °C, 30 s at 50 °C, and 1 min at 68 °C). Products were then ligated into the pGEM T-easy vector (Promega, Madison, WI), transformed into *Escherichia coli* (JM109 strain) and plasmids purified with the QIAprep Spin Miniprep Kit (Qiagen, Valencia, CA). Clones containing inserts were sequenced using the Big Dye Terminator 3.1 Cycle Sequencing Kit (Applied Biosystems, Foster City, CA). The 5′-RACE products were obtained by designing species-specific primers (available upon request) from 3′-RACE products. Products were amplified using the touchdown PCR protocol specified with the BD Advantage Polymerase Kit (BD Biosciences, San Jose, CA).

Genomic DNA was extracted from an additional 12 nymphalid species (*Asterocampa celtis*, *A. demophon*, *H. charithonia*, *Marpesia chiron*, *Marpesia orsilochus*,

Table 1
Taxonomic Distribution of Long-Wavelength (L) Opsin Sequences and Absorbance Spectrum Maxima (λ_{max}) Used in This Study

Family	Subfamily	Taxon and Sequence	Locality	GenBank Accession Number	Sample[a]	λ_{max} (nm)
Lycaenidae	Lycaeninae	*Lycaena rubidus*		AY587901	—	568[b]
Nymphalidae	**Apaturinae**	***Asterocampa celtis***	Florida: Gainesville	**DQ924362**	**F-20**	**530**[c]
Nymphalidae	**Charaxinae**	***Archaeoprepona demophon***	Brazil: Rondonia	**DQ924363**	**RB-263**	**565**
Nymphalidae	**Cyrestinae**	***Marpesia chiron***	Brazil: Rondonia	**DQ924364**	**RB-227**	—
Nymphalidae	**Cyrestinae**	***Marpesia orsilochus***	Brazil: Rondonia	**DQ924365**	**RB-250**	—
Nymphalidae	Danainae	*Danaus plexippus*		AY605541	CAL-22	545
Nymphalidae	**Heliconiinae**	***Agraulis vanillae***	California: Huntington Beach	**DQ924367**	**AVAN**	**555**
Nymphalidae	Heliconiinae	*Dryas iulia*		AF126757	—	—
Nymphalidae	**Heliconiinae**	***Heliconius charithonia***		**EF666488**	—	**550**
Nymphalidae	Heliconiinae	*Heliconius cydno*		AF126755	—	—
Nymphalidae	Heliconiinae	*Heliconius erato*		AY918907	—	555
Nymphalidae	Heliconiinae	*Heliconius hecale*		N/A	—	560
Nymphalidae	Heliconiinae	*Heliconius hewitsoni*		AF126752	—	—
Nymphalidae	Heliconiinae	*Heliconius melpomene*		AF126751	—	—
Nymphalidae	Heliconiinae	*Heliconius pachinus*		AF126756	—	—
Nymphalidae	Heliconiinae	*Heliconius sapho*		AF126754	—	—
Nymphalidae	Heliconiinae	*Heliconius sara*		AF126753	—	550
Nymphalidae	**Heliconiinae**	***Philaethria dido***	Panama: Canal zone	**DQ924368**	**P7-4**	—
Nymphalidae	**Heliconiinae**	***Speyeria mormonia***	California: Mono Co.	**DQ924366**	**SMOR**	—
Nymphalidae	**Libytheinae**	***Libytheana carinenta***	Brazil: Rondonia	**DQ924369**	**RB-253**	—
Nymphalidae	**Limenitidinae**	***Adelpha bredowi***	Arizona: Cochise Co.	**DQ212967**	**AZ-1-07**	—
Nymphalidae	Limenitidinae	*Limenitis archippus archippus*		DQ212963	—	514[d]
Nymphalidae	Limenitidinae	*Limenitis archippus floridensis*		DQ486871	—	514[d]
Nymphalidae	Limenitidinae	*Limenitis arthemis astyanax*		DQ212962	—	545[d]
Nymphalidae	Limenitidinae	*Limenitis lorquini*		DQ212965	—	530[d]
Nymphalidae	Limenitidinae	*Limenitis weidemeyerii*		DQ212966	—	530[d]
Nymphalidae	**Morphinae**	***Morpho helenor***	Brazil: Rondonia	**DQ924370**	**RB-228**	—
Nymphalidae	**Morphinae**	***Amathusia phidippus LWRh1***	Malaysia: Sabah	**DQ924371**	**SA-2-6**	—
Nymphalidae	**Nymphalinae**	***Anartia jatrophae***	Brazil: Rondonia	**DQ924372**	**RB-374**	**530/565**[e]
Nymphalidae	**Nymphalinae**	***Euphydryas chalcedona***	California: Mono Co.	**DQ924373**	**ECAL**	**565**
Nymphalidae	Nymphalinae	*Inachis io*		AY740906	—	530[f]
Nymphalidae	Nymphalinae	*Junonia coenia*		AF385332	—	510[f]
Nymphalidae	Nymphalinae	*Nymphalis antiopa*		AY740907	—	534[f]
Nymphalidae	Nymphalinae	*Siproeta stelenes*		AY740908	—	522[f]
Nymphalidae	Nymphalinae	*Vanessa cardui*		AF385333	—	530[g]
Nymphalidae	**Satyrinae**	***Bicyclus anynana***		**AY918895**	**BAN**	—
Nymphalidae	**Satyrinae**	***Coenonympha tullia***	Colorado: Boulder	**DQ924374**	**CTUL**	—
Nymphalidae	**Satyrinae**	***Hermeuptychia hermes LWRh1, LWRh2***	Florida: Gainesville	**DQ924375, DQ924376**	**F-25**	**530**[e]
Nymphalidae	**Satyrinae**	***Neominois ridingsii***	Colorado: Montrose Co.	**DQ924377**	**NRID**	**515**
Nymphalidae	**Satyrinae**	***Oeneis chryxus***	Colorado: Boulder	**DQ924378**	**OXUS**	**530**
Papilionidae	Papilioninae	*Papilio glaucus PglRh1–PglRh3*		AF077189, AF077190, AF098283	—	—
Papilionidae	Papilioninae	*Papilio xuthus PxRh1–PxRh3*		AB007423-AB007425	—	530/515/575[h]
Pieridae	Pierinae	*Pieris rapae*		AB188567	—	563[i]
Riodinidae	**Riodininae**	***Apodemia mormo LWRh1, LWRh2***		**AY587907, AY587908**	**APO**	**505/600**[e,j]
Sphingidae	Sphinginae	*Manduca sexta*		L78080		520 nm[k]

NOTE.—New sequences are in bold.
[a] Source animal used to determine opsin genotype.
GenBank accessions and λ_{max} values from:
[b] Bernard and Remington (1991).
[c] λ_{max} was measured from *Asterocampa leilia*.
[d] Frentiu et al. (2007).
[e] λ_{max} value could not be assigned to a specific L opsin.
[f] Briscoe and Bernard (2005).
[g] Bernard (1983).
[h] Arikawa et al. (2003).
[i] Wakakuwa et al. (2004).
[j] Bernard et al. (1988).
[k] White et al. (1983).

Philaethria dido, *Libytheana carinenta*, *Adelpha bredowi*, *Morpho helenor*, *A. phidippus*, *A. jatrophae*, and *H. hermes*) using a standard phenol–chloroform method. A region of approximately 300 bp of the opsin gene was amplified for each species using the same degenerate primer pair as above and a reverse primer (5′-CCR TAN ACR ATN GGR TTR TA-3′) with the following PCR conditions: 94 °C for 1 min, then 35 cycles of 94 °C for 30 s, 50 °C for 1 min, and 68 °C for 10 min. PCR products were gel-purified, cloned, and sequenced as described above. Sequences served as templates for the design of species-specific reverse primers, which were then used with another degenerate primer

(5′-CAY YTN ATH GAY CCN CAY TGG-3′). The fragment was then cloned and sequenced as above. Sequences were aligned, edited, and the introns manually removed using SeqMan in the Lasergene package (DNASTAR, Madison, WI).

Phylogenetic Inference

First, to test the utility of L opsin genes for assessing evolutionary relationships among butterfly families, phylogenetic hypotheses were inferred using full-length cDNAs for a set of 22 species (a total of 1152 bp). Second, in order to map spectral shifts in absorbance spectrum maximum across butterflies, phylogenetic relationships among L visual pigment lineages were inferred from nucleotide data for a set of 28 pigments for which both opsin sequence (795 bp of coding region) and λ_{max} values were available (table 1 and supplementary fig. 1 [Supplementary Material online]). Lastly, we determined phylogenetic relationships among all available butterfly L opsins also using 795 bp of opsin-coding sequence (alignment shown in supplementary fig. 1, Supplementary Material online). All analyses were conducted on all codon positions, and Modeltest (Posada and Crandall 1998) as implemented in HYPHY (Kosakovsky-Pond et al. 2005) was used to determine the best-fit DNA substitution model for a maximum likelihood (ML) analysis using the Akaike information criterion. ML analysis was conducted in PHYML (Guindon and Gascuel 2003) with the GTR + I + G (invariant sites and gamma-distributed rates for sites) model, and the reliability of the tree was tested using 500 bootstrap replicates. Bayesian phylogenetic analysis was performed in MrBayes 3.1 with the GTR + I + G nucleotide substitution model, with 2 heated chains for 2×10^6 generations, and with a sampling frequency of 10^2 and a burn-in of 5×10^3 trees.

Character Mapping of Spectral Shifts and Ancestral State Reconstructions

The physiological diversity of butterfly L photopigment λ_{max} values observed (table 1) suggested that adaptive evolution has played a significant role in their evolution. We were specifically interested in examining the hypothesis that amino acid substitutions at 4 sites (17, 64, 70, and 137) previously shown to be under positive selection in the *Limenitis* L opsins (Frentiu et al. 2007) may be correlated with the spectral diversification of L photopigments in this expanded data set. To test this hypothesis, we took 2 approaches. First, we mapped photopigment λmax values onto an L opsin phylogeny in order to correlate shifts in spectral phenotype with particular amino acid changes. Ancestral states at these 4 sites were also reconstructed for all available L opsins ($N = 49$) and mapped onto a phylogenetic tree to infer the frequency of their occurrence. Ancestral amino acids along each node in the phylogeny were inferred using maximum parsimony (MP) and ML methods in MacClade (Maddison DR and Maddison WP 2005) and CodonML in the PAML 3.15 package (Yang 1997), respectively.

Second, ancestral L photopigment λ_{max} values were inferred using least-squares MP in the Mesquite package (Maddison WP and Maddison DR 2005). ML ancestral inferences, including the standard error (SE) estimates (equivalent to the standard deviation [SD] of the marginal distribution of the ML estimate; see Schluter et al. 1997) were performed in the program ANCML assuming a Brownian-motion model of evolution of continuously distributed characters. We note that both programs assume that proteins or phenotypic character states evolve in an additive manner, which is an assumption that is difficult to test directly. Our data must therefore be viewed in the context of this assumption.

Relative Rates Tests

We discovered 2 instances of lineage-specific gene duplication in the Nymphalidae (*H. hermes*, a member of the subfamily Satyrinae, and *A. phidippus*, a member of the subfamily Morphinae, table 1) and 1 instance in the Riodinidae (*A. mormo*). The 2 *A. phidippus* L opsin copies differed by 24 out of 300 bp (8%) of coding region (supplementary fig. 2, Supplementary Material online) and contained 2 introns of variable length. However, because we were unable to obtain more coding sequence from *A. phidippus* LWRh2, this gene was not used in further analyses. The hypothesis that duplicates may not be evolving at the same pace was investigated using phylogeny-based relative rates tests. Tests were conducted in the program RRTree (Robinson-Rechavi and Huchon 2000) on the *H. hermes* and *A. mormo* duplicates, with *B. anynana* and *P. rapae* as outgroups, respectively.

Homology Modeling

We employed homology modeling to investigate the structural proximity of specific amino acid residues to the chromophore because the mechanisms of spectral tuning of insect photopigments are poorly understood (Britt et al. 1993; Salcedo et al. 2003). Because the majority of L opsin sequences used in this study are from nymphalid butterflies, we used the *L. a. astyanax* L opsin homology model of Frentiu et al. (2007), which is based on the crystal structure of bovine rhodopsin (Palczewski et al. 2000; Okada et al. 2004) to map sites that appear to change frequently either in parallel or convergently among lepidopteran opsins correlated with spectral shifts in L photopigment absorbance (supplementary fig. 3, Supplementary Material online).

Results and Discussion

Molecular studies of the nymphalid butterflies *D. plexippus* and *V. cardui* have shown that the UV-, B-, and L-sensitive photopigments are encoded by 1 UV, 1 B, and 1 L opsin gene likely present in the ancestor of all butterflies and moths. In the main retina of these species, the R1 and R2 photoreceptor cells express either UV or B opsin mRNAs and the R3-8 photoreceptors express the L opsin mRNA (Briscoe et al. 2003; Sauman et al. 2005). (R9 has only been examined in *V. cardui*, and this cell expresses the same L opsin mRNA as the R3-8 photoreceptor cells

[Briscoe et al. 2003].) This basic pattern of opsin expression within nymphalids, together with the presence of a tapetum, makes it possible to link the L photopigment absorbance spectra measured by microspectrophotometry to the L opsin gene sequences (see below).

Extensive Phenotypic Diversity of Butterfly L Visual Pigments

Our study represents the most taxonomically comprehensive investigation to date of the distribution of L photopigment spectra in butterflies measured microspectrophotometrically. Extensive spectral diversity at several taxonomic levels exists in these pigments, as the range of absorbance spectrum maxima (most estimates accurate to approximately ±1.5 nm) for 22 species indicates (fig. 1). For each of the 3 subfamilies, Apaturinae, Charaxinae, and Danainae, we obtained λ_{max} measurements from 1 exemplar: *A. leilia* (530 nm), *A. demophon* (565 nm), and monarch *D. plexippus* (545 nm) (fig. 1*A–C*). We note that the 545 nm estimate for the L photopigment of monarch is in good agreement with the 540 nm estimate obtained from intracellular recordings (Stalleicken et al. 2006).

Variation of λmax within the subfamily Nymphalinae was as wide as the variation we observed across the entire Nymphalidae family and ranged from λ_{max} = 510 nm in the buckeye *J. coenia* (Briscoe and Bernard 2005) to λ_{max} = 565 nm in *A. jatrophae* (fig. 1*F*). Within nymphalids, we found photochemical evidence of only 1 L photopigment in all but 1 species, *A. jatrophae*, where in addition to the 565-nm pigment we found evidence of a 530-nm pigment. Even further blue and redshifted L visual pigments existed in the Riodinidae, with the metalmark butterfly *A. mormo* having 2 pigments with peak absorbance at 505 and 600 nm, respectively (fig. 1*H*). Indeed, a survey of insect L visual pigments that have been studied photochemically indicated that the *A. mormo* 600-nm value is the most redshifted λmax yet reported in any butterfly (reviewed in Briscoe and Chittka 2001).

Significant spectral diversity was observed within 2 other nymphalid subfamilies, the Satyrinae and the Limenitidinae (fig. 1*G* and *E*, respectively). For Satyrinae, λmax ranged from 515 nm in *N. ridingsii* to 530 nm in *O. chryxus*. Interestingly, we found photochemical evidence of only one L pigment in the eye of the satyrine *H. hermes* (λ_{max} = 530 nm), even though we did clone 2 L opsin genes in this species (potential reasons for this discrepancy are discussed below). As mentioned previously, there was a 31-nm range of spectral diversity in the L photopigments of North American *Limenitis* species (fig. 1*E*; λ_{max} = 514–545 nm; Frentiu et al. 2007).

In contrast to *Limenitis*, none of the L photopigments sampled within the genus *Heliconius* (i.e., *H. erato*, *H. charithonia*, and *H. hecale*) showed evidence of significant physiological diversification (fig. 1*D*; λ_{max} = 550–560 nm). Both the North American *Limenitis* and the 2 principal *Heliconius* clades diverged ~ 4 MYA (Brower 1994; Mullen 2006), and both groups are known for their mimicry-driven diversification of wing patterns. However, evolution of L visual pigment λmax has proceeded at different paces in the 2 groups, suggesting factors other than mimicry-related wing change are mediating visual pigment absorbance spectra, at least in *Heliconius*.

L Opsin Gene Tree Recovers Familial-Level Relationships

Full-length coding L opsin cDNAs (encoding 380–384 amino acids) were obtained from 8 species. Using these data along with full-length coding sequences from GenBank, we investigated the utility of L opsins for reconstructing the broad phylogenetic relationships within Lepidoptera using ML and Bayesian inference. Despite the sparse sampling of most genera within families, most nodes were well supported (>50%; fig. 2) and the overall phylogeny was similar to other trees obtained from blue opsins (Sison-Mangus et al. 2006) and other nuclear and mitochondrial genes (Brower 2000; Wahlberg et al. 2003, 2005). Most butterfly families appeared as monophyletic clades, except for Lycaenidae and Riodinidae in which a duplicate L opsin (LWRh1) was evident in the riodinid *A. mormo* and was not found in the lycaenid *L. rubidus*. This unusual relationship may reflect the difficulty in resolving relationships between the 2 sister groups based on single exemplars (Wahlberg et al. 2005). Alternatively, the ancestral opsin may have duplicated prior to the split between the lycaenid and riodinid lineages and 1 copy (*LWRh1*) was lost in the lycaenids.

Ancestral Nymphalid L Photopigment λ_{max} Estimates and Inferred Blue Spectral Shifts

For the remaining nymphalid species in this study, we obtained between 1365–3012 bp of L opsin sequence from genomic DNA, including coding sequence for 266 amino acids spanning 6 transmembrane domains (supplementary fig. 1, Supplementary Material online). Using these data, we investigated the pattern of L photopigment spectral shifts among butterflies by mapping all λmax values available onto an L opsin phylogeny (fig. 3). Both Bayesian and ML analyses returned the same topology, but most nodes received higher support in the Bayesian analysis. Separate MP and ML methods returned estimates of λ_{max} values for L photopigments at ancestral nodes that were in good agreement with each other. The most parsimonious λ_{max} estimates at nodes 1, 2, and 3 (fig. 3) were 542 nm, 540 nm, and 537 nm, respectively. ML estimates and their SE estimates (equivalent to the SD of the marginal distribution of the ML estimate; see Schluter et al. 1997), at the same nodes were 540 nm (±10 nm), 539 nm (±9 nm), and 541 nm (±13 nm). The estimated values at nodes 1 and 2 (fig. 3) suggest that the ancestral nymphalid L photopigment λ_{max} was ~540 nm (nodes 1 and 2, fig. 3). Interestingly, this ancestral state estimate is similar to the mean λ_{max} = 534 nm (SD ± 10 nm) of L photoreceptors measured from 46 extant bee species (Peitsch et al. 1992).

From these data, we propose that blueshifts in peak absorbance from the ancestral nymphalid L photopigment λ_{max} value of 540 ± 10 nm to λ_{max} approximately ≤530 nm have evolved in 4 lineages within the Nymphalidae (fig. 3). (We chose to categorize blueshifted pigments as having λ_{max} approximately ≤530 nm due to the uncertainty in the

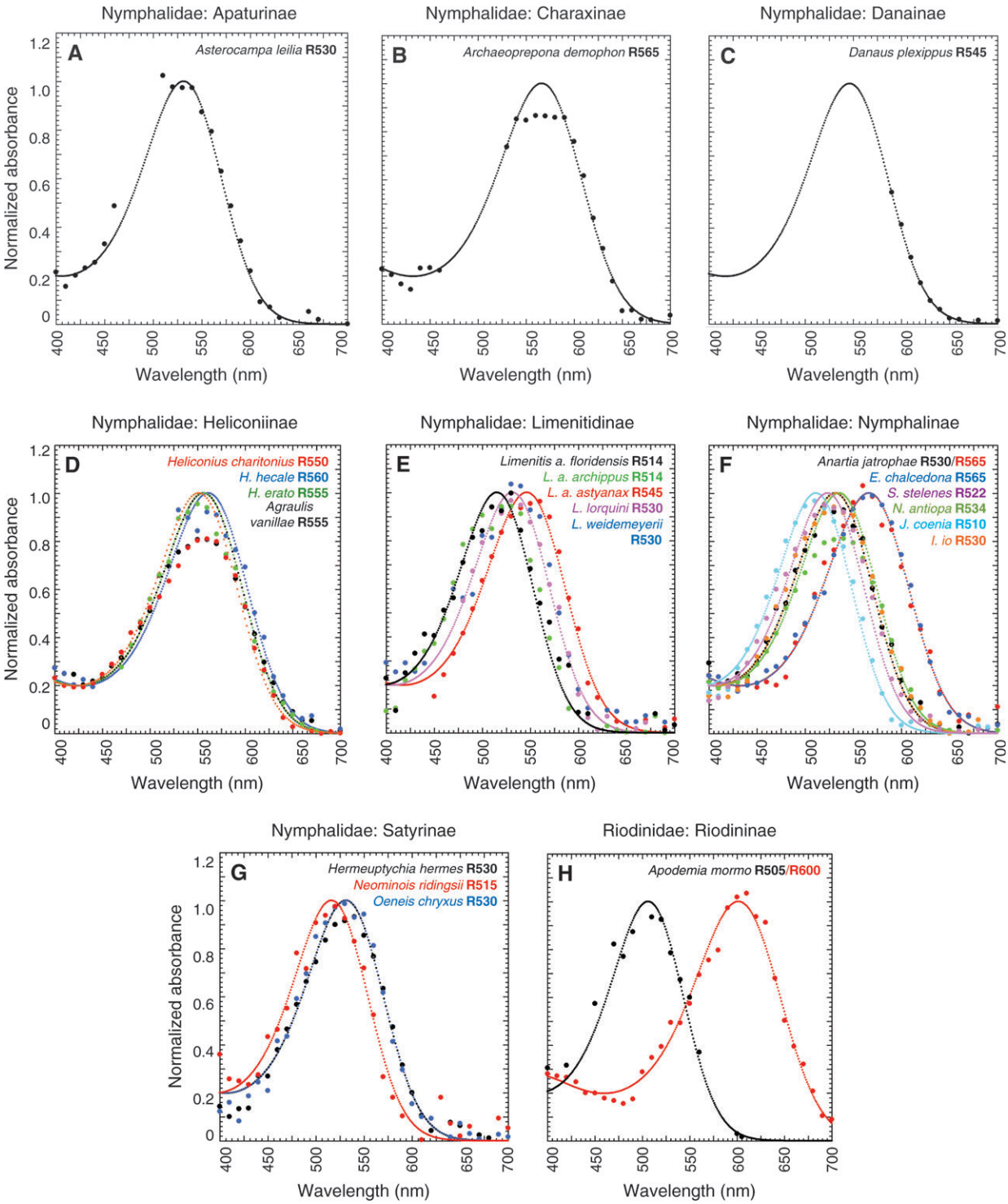

FIG. 1.—Normalized absorbance spectra of 22 L photopigments across 7 subfamilies in the Nymphalidae and 1 in the Riodinidae. Idealized spectra (solid curves) based on the Bernard (1987) template. Species names and λ_{max} estimates (accurate to ca. ±1.5 nm, see supplementary Materials and Methods, Supplementary Material online for details) are shown in upper right hand corner. Spectra for Limenitidinae species (*E*) reprinted from Frentiu et al. (2007). Spectra for *Nymphalis antiopa*, *Siproeta stelenes*, *Junonia coenia*, and *Inachis io* (*F*) reprinted as normalized spectra from Briscoe and Bernard (2005).

estimate of the ancestral L photopigment λ_{max} values.) To more rigorously define blue spectral shifts, we examined ancestral λ_{max} values at all nodes in the tree. Blueshifts were inferred from the branch leading from node A (λ_{max} = 536 ± 4 nm) to node B (λ_{max} = 530 ± 2 nm) (error estimates as noted above are equivalent to the SD of the marginal distribution of the ML estimate); from node C (λ_{max} = 534 ± 7 nm) to node D (λ_{max} = 529 ± 7); from

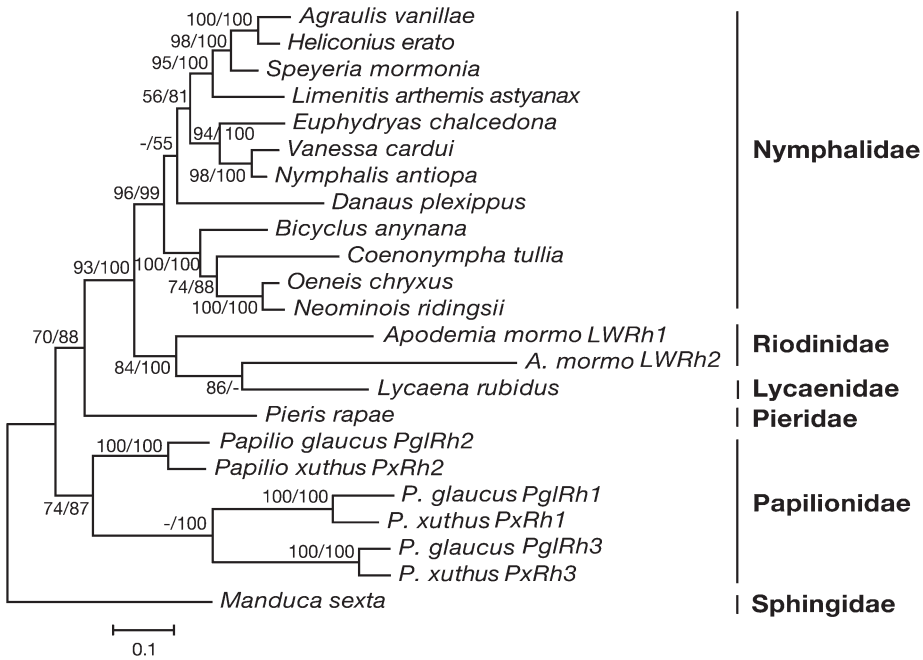

FIG. 2.—Phylogenetic relationships among lepidopteran L opsins based on full-length cDNAs inferred using ML and Bayesian methods, under a GTR + I + G model. ML bootstrap values ($N = 500$) and Bayesian clade credibility values given as percentage before and after the slash, respectively. Branch lengths are proportional to the number of substitutions per site, as indicated by the scale bar.

node E ($\lambda_{max} = 539 \pm 7$ nm) to node F ($\lambda_{max} = 533 \pm 6$ nm); and from node G ($\lambda_{max} = 542 \pm 10$ nm) to node H ($\lambda_{max} = 528 \pm 5$ nm), which was at the base of the clade comprising *N. ridingsii* and *O. chryxus* (fig. 3). A further blueshift was inferred from node D ($\lambda_{max} = 529 \pm 7$ nm) to the branch leading to *J. coenia*, $\lambda_{max} = 510$ nm (fig. 3; see table 2 below). These data also suggest that the *A. mormo* photopigment with $\lambda_{max} = 505$ nm (LWRh1) was likely blueshifted compared with its 540 ± 13-nm ancestor (results not shown).

Amino Acid Substitutions Correlated with Blue Spectral Shifts

Along the same pigment lineages, parallel and convergent amino acid substitutions were inferred to have also occurred in the L opsins in tandem with spectral shifts (table 2). Some of the same amino acid sites previously found to be under positive selection in *Limenitis* L photopigments (sites 64, 70, and 137; Frentiu et al. 2007) were found in this expanded analysis as well as several new sites. A total of 10 sites (positions 26, 64, 70, 131, 137, 145, 165, 170, 177, and 260; supplementary fig. 1, Supplementary Material online) displayed parallel amino acid substitutions along at least 2 lineages and 2 sites (61 and 177) displayed convergent evolution. Along the branches connecting nodes E to F and nodes G to H on the tree shown in figure 3, 3 sites had acquired parallel substitutions (Ala64Ser, Phe131Leu, and Phe165Leu), which were more sites than expected by chance ($P < 0.000$) using the method of Zhang and Kumar (1997) (table 2). Site 177 is in transmembrane domain V facing outward though in the same plane as the chromophore such that it might influence spectral tuning via steric effects, and site 165 is in extracellular loop domain II that folds deep into the chromophore-binding pocket of bovine rhodopsin (Palczewski et al. 2000). All other sites (26, 131, 145, 170, and 260), except for sites 64, 70, and 137 as previously reported (see below) (Frentiu et al. 2007), are further removed from the chromophore.

Most strikingly, the Ala to Ser substitution at site 64 was associated with at least 4 phylogenetically independent blueshifts (table 2). Using a homology model of a nymphalid opsin protein, we previously found that site 64 was located immediately adjacent (within 5 Å) to the chromophore, suggesting a principal spectral tuning role for this site (Frentiu et al. 2007). A Pro91Ser mutation in its bovine rhodopsin equivalent causes a shift of 10 nm toward the blue in vertebrate short wavelength–sensitive visual pigments (Takahashi and Ebrey 2003). Mutagenesis experiments using native butterfly pigments as a template are needed to confirm the hypothesized spectral tuning effects of the Ala to Ser substitution at site 64.

Mapping of Substitutions at Candidate Spectral Tuning Sites Indicates Frequent Shifts in λ_{max}

Vertebrate middle- and long-wavelength (MWS and LWS, respectively) visual pigment spectra can be determined by inspecting amino acids present at 5 sites within the opsin (Merbs and Nathans 1992; Asenjo et al. 1994; Yokoyama and Radlwimmer 1998, 1999). Assuming effects are roughly additive, concordance between particular amino acid residues at butterfly opsin site 64 and blue spectral shifts suggests that it may be possible to use this site to

Table 2
ML and MP Ancestral State Reconstructions of Amino Acid Residues at Key Nodes Shown in Figure 3

AA Site	536 ± 4 nm Node A	530 ± 2 nm Node B	AA Site	534 ± 7 nm Node C	529 ± 7 nm Node D	AA Site	529 ± 7 nm Node D	510 nm *Junonia coenia*	AA Site	539 ± 7 nm Node E	533 ± 6 nm Node F	AA Site	542 ± 10 nm Node G	528 ± 5 nm Node H
6	N 0.993	D 1.000	18	G 0.980	A 0.635	8	L 0.992	M	16[a]	F 0.846	V 0.994	2	F 0.998	Y 1.000
26[a]	A 0.542	T 0.519	**137**	**S 0.998**	**A 0.985**	20	L 1.000	I	19[a]	V 0.768	I 0.990	**26**[a]	**T 0.628**	**A 0.990**
64	**A 0.930**	**S 0.998**	142	V 0. 553	L 0.904	**26**	**T 0.977**	**A**	32[a]	V 0.848	I 0.677	***61***	***L 0.549***	***T 0.991***
70	**N 0.993**	**S 1.000**	**145**[b]	**L**	**M**	40[a]	*T 0.550*	*S*	61[a]	F 0.299	C 0.997	**64**	**A 0.967**	**S 0.996**
137	**S 0.995**	**A 1.000**	168[b]	S	T	***61***	***L***[b]***/F***[a] ***0.413***	***T***	**64**	**A 0.988**	**S 0.996**	**131**[a]	**F 0.720**	**L 1.000**
177[a]	***F 0. 557***	***V 0.997***	**177**[a]	**L 0.646**	**I 0.635**	**64**	**A 0.982**	**S**	73[a]	Y 0.669	N 0.879	**145**	**L 0.901**	**M 0.991**
			260	**A 0.953**	**S 0.681**	**70**	**N 0.999**	**S**	127	L 1.000	M 1.000	**165**[a]	**F 0.897**	**L 1.000**
						93	F 0.999	C	**131**	**F 0.995**	**L 1.000**	***177***[a]	***L 0.800***	***V 0.987***
						170[a]	**L 0.938**	**F**	**165**	**F 1.000**	**L 1.000**	185	A 0.890	S 0.996
						180	V 0.975	L	**170**[a]	**L 0.938**	**F 0.987**	**260**	**A 0.896**	**S 0.993**
									177[a]	**L 0.687**	**I 0.891**			

NOTE.—Numbers above the nodes are ML reconstructions of λ_{max} values and their standard errors. Amino acid (AA) sites changing in parallel or convergently between nodes are shown in bold and bolded italics, respectively, along with Bayesian posterior probabilities for each reconstruction. Numbering of sites is with respect to alignment shown in supplementary figure 1 (Supplementary Material online).

[a] Changes detected via ML only.

[b] Changes detected via MP only.

predict spectral shifts in nymphalid L photopigments in which physiological information is lacking, as is currently possible for vertebrate MWS and LWS visual pigments (Yokoyama 2000). The pattern of change in absorbance spectra observed in the L visual pigment phylogeny (fig. 3) suggested that shifts in λmax occur frequently in butterflies. To evaluate this hypothesis, we reconstructed phylogenetic relationships across all 49 butterfly L opsin sequences available and then mapped amino acid substitutions at key candidate spectral tuning sites found in this (i.e., site 64) and previous analyses (sites 17, 64, 70, and 137; Frentiu et al. 2007) (Briscoe and Bernard 2005).

Phylogenetic relationships among the 49 taxa as indicated by L opsins were generally in agreement with previously published evolutionary relationships (Brower 2000; Wahlberg et al. 2003, 2005), with most nymphalid subfamilies forming well-supported monophyletic groups (fig. 4). The Satyrinae was found to be polyphyletic, with members of the subfamilies Morphinae and Charaxinae clustering within this group (fig. 4), reflecting the close relationship among these groups reported previously (Wahlberg et al. 2003; Peña et al. 2006). However, our phylogenetic tree suggested that the Danainae is not the basal nymphalid family, as implied by other genes (Wahlberg et al. 2003, 2005). This pattern may reflect the fact that our phylogeny is a single-gene tree because the position of the Danainae in other studies also changes depending on which gene is used to reconstruct evolutionary relationships (Wahlberg et al. 2005).

Mapping of amino acid substitutions onto the expanded L opsin phylogeny indicated that there have been multiple occasions of parallel changes at key spectral tuning sites implicated in blue spectral shifts (fig. 4): Ile17Met occurred 5 times (open red circles), Asn70Ser occurred 3 times (purple), and Ser137Ala occurred 3 times (yellow dots). Most striking, however, was the frequency of the Ala64Ser substitution, which occurred 8 times across the whole tree (fig. 4, blue dots). Because site Ala64Ser is strongly associated with shifts in λmax toward the blue, the pattern observed suggests that these types of shifts occur commonly in the Nymphalidae.

We also observed an intriguing pattern of reverse substitution at 2 key putative spectral tuning sites. The Ser64-Ala change occurred 2 times (open blue circles) and was associated with an L pigment showing a redshift in λmax as in *L. a. astyanax* (fig. 4). The Met17Ile substitution also occurred twice (fig. 4, red dots), including a branch in which there was a red spectral shift because both *A. jatrophae* and *E. chalcedona* had $\lambda_{max} = 565$ nm, but the ancestral pigment may have had $\lambda_{max} = 534 \pm 7$ nm (results not shown). These patterns indicate that the reverse mutation may result in the opposite spectral shift and have a symmetrical effect, at least qualitatively. For example, the substitution A269T in bovine rhodopsin shifts the λ_{max} by 14 nm toward the red (Chan et al. 1992), but the reverse substitution at the corresponding site in human L pigments causes a 16-nm blueshift (Asenjo et al. 1994).

Given the strong associations between key sites and spectral shifts, it may be possible to use ancestral reconstructions and the presence of particular amino acid residues at these sites to predict shifts absorbance spectra in

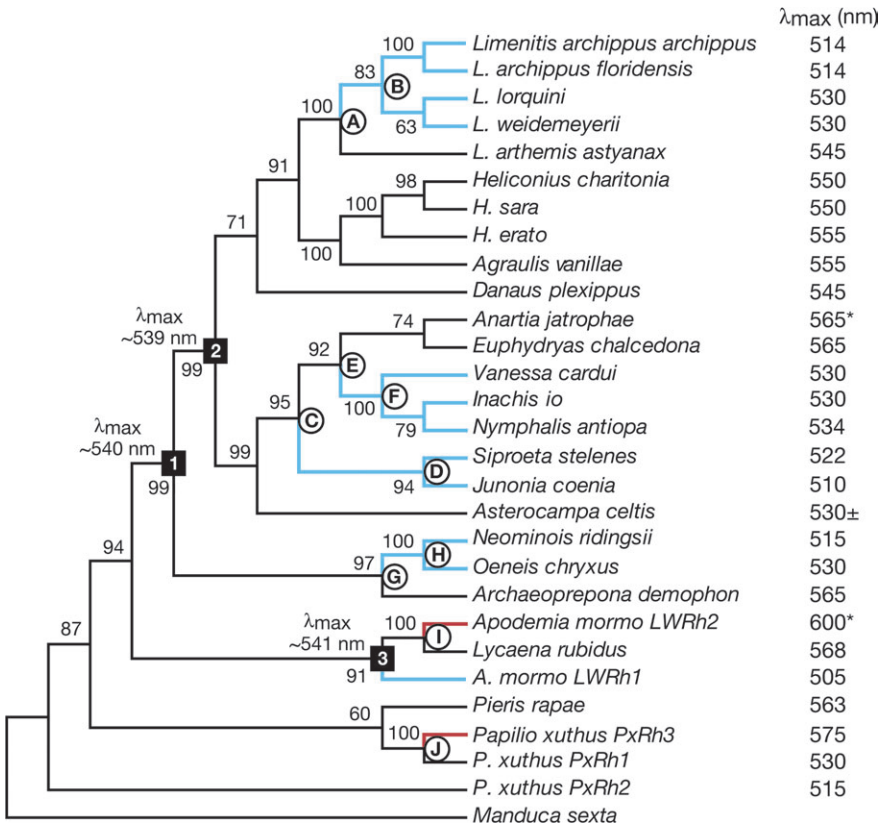

FIG. 3.—Evolution of butterfly L photopigment absorbance spectra (λ_{max}). Phylogenetic relationships inferred from L opsin genes and using ML and Bayesian methods (GTR + I + G model; Bayesian clade credibility values >50% shown as percentages). Branches displaying shifts in absorbance spectra toward the longer wavelengths are shown in red and branches denoting shifts in spectral peak toward the shorter wavelengths are shown in blue. Letters within circles define nodes connected by branches that display parallel and convergent amino acid changes occurring in tandem with similar shifts in spectral peak. Numbers denote nodes where ancestral L photopigment λ_{max} was reconstructed and only ML reconstructions are shown. The symbol ± indicates λ_{max} determined for congener *Asterocampa leilia*. Asterisk indicates that because *Anartia jatrophae* and *Apodemia mormo* LWRh2 pigments cluster with others that are redshifted, it is most likely that these pigments have λ_{max} values that are 565 and 600 nm, respectively.

taxa whose spectra have not yet been measured. But these predictions can only be clarified once the hypothesized spectral tuning effects of these substitutions have been validated by site-directed mutagenesis and functional characterization. For example, an Ala64Ser substitution occurred along the branches leading to the *Marpesia* opsins and the *A. phidippus* LWRh1 opsin, implying that the visual pigments may be blueshifted in sensitivity (fig. 4). Similarly, the substitution Ser137Ala occurred along the branch leading to *M. helenor* (fig. 4), suggesting that photo pigment may also blueshifted. Although in vitro mutagenesis studies are needed to test the hypothesized spectral tuning effect of these sites, in vivo physiological data on the λ_{max} values of L pigments in species like *A. phidippus* and *M. helenor* provides an additional, complementary test.

Parallel Evolution of Red-Sensitive Photoreceptors through Gene Duplication

Our sequence data indicate that L opsin gene duplication has occurred several times in butterflies. Independent duplicates were found in 3 new species: *A. phidippus*, *A. mormo*, and *H. hermes*, showing that L opsin gene duplication has occurred in 3 out of 5 butterfly families (Briscoe 1998; Kitamoto et al. 1998). Physiological data revealed the presence of 2 L visual pigments in the nymphaline species *A. jatrophae* (fig. 1*F*), but we were unable to isolate a second L opsin gene from genomic DNA. Either we missed a second L opsin gene in our screen or the 530-nm photopigment is encoded by a different opsin gene family member, such as by a duplicate blue opsin gene, for which we did not screen. Precedent for such a pigment has been found in the lycaenid *L. rubidus*, in which a 500-nm photopigment is encoded by a blue opsin (Sison-Mangus et al. 2006). A screen of additional samples, including eye-specific cDNA, may help resolve this issue.

Curiously, we discovered the presence of 2 L opsin genes in *H. hermes* but only identified physiologically 1 L visual pigment in the eye (fig. 1*G*). The amino acid sequences of the *H. hermes* duplicate genes suggest that both copies are functional opsins (supplementary fig. 1, Supplementary Material online). The absence of a second L visual pigment in the eye suggests that the second *H. hermes* opsin is expressed in another body tissue, such as the brain, as has been found in *Papilio glaucus* (Briscoe 2000) and moths (Shimizu et al. 2001; Lampel et al. 2005).

Duplicate copies of the *H. hermes* and *A. mormo* L opsins have evolved at significantly different rates (table 3),

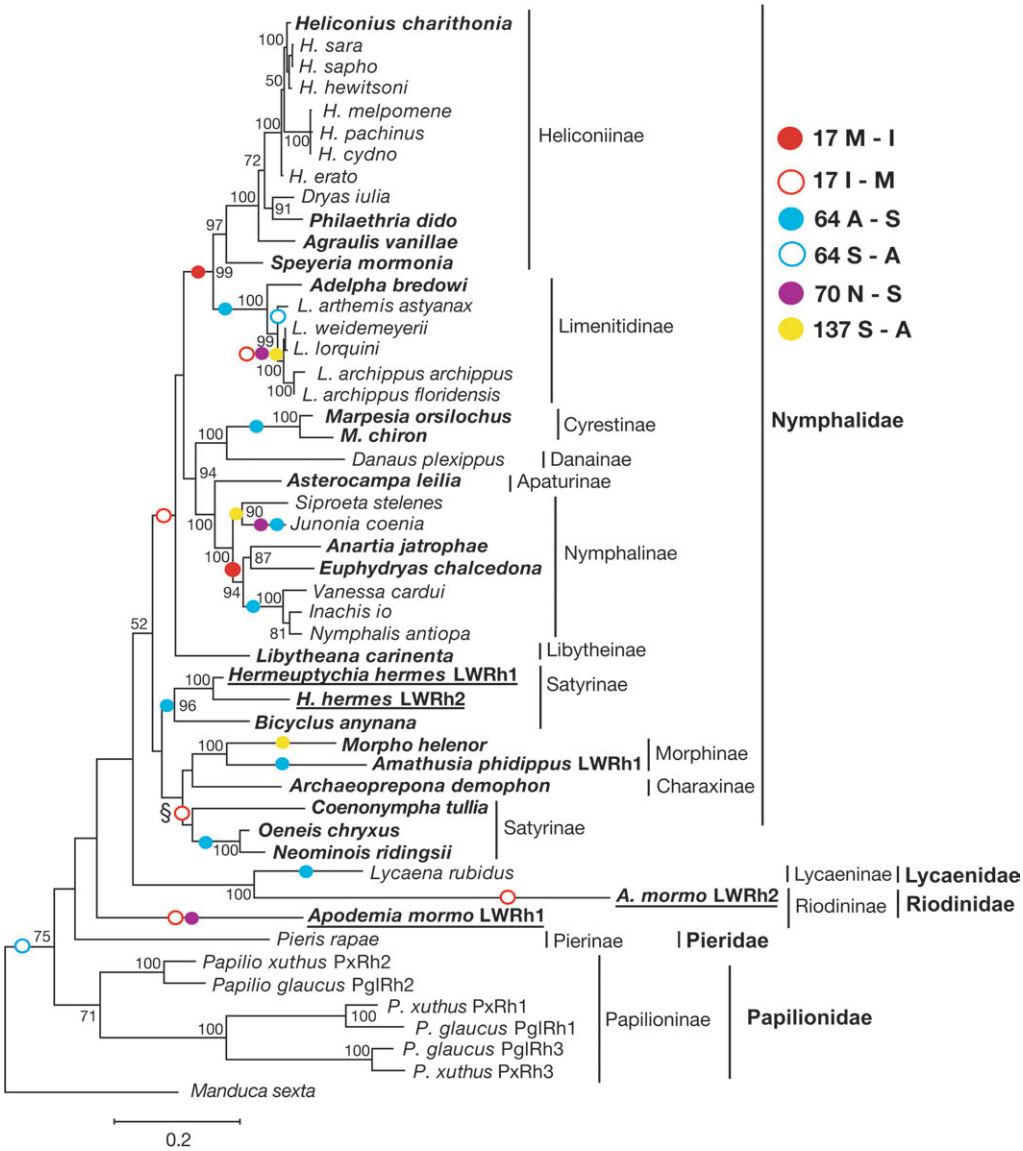

FIG. 4.—Distribution of amino acid changes at sites located near the chromophore in a set of 49 lepidopteran L opsins. Tree shown is based upon ML analysis of 795 bp using the GTR + I + G model. Ancestral amino acid states were reconstructed via the likelihood method using the ML phylogeny. Numbers at each node represent Bayesian clade credibility values >50%. The symbol § indicates Bayesian topology fails to resolve this node. Sequences contributed by this study shown in bold. Newly identified duplicate genes are underlined.

particularly at nonsynonymous codon sites. Interestingly, *A. mormo* LWRh2 appears to have evolved much faster than the *A. mormo* LWRh1 opsin at nonsynonymous ($P < 0.002$) rather than synonymous sites ($P = 0.538$). This pattern of evolution suggests strong diversifying selection acting on the LWRh2 copy and is consistent with it encoding the 600-nm photopigment.

The presence of *P. xuthus* and *A. mormo* visual pigments with $\lambda_{max} = 575$ nm and $\lambda_{max} = 600$ nm, respectively, and their independent origin (fig. 3), indicates the parallel evolution in the Papilionidae and Riodinidae families of photoreceptors, which are considerably redshifted compared with their ancestral pigments, and compared with the most redshifted photopigment observed in nymphalids (565 nm). Interestingly, the far redshifted photopigments are both encoded by independently arising duplicate opsin gene copies (fig. 2). More strikingly, the evolution of these parallel spectral phenotypes has been accompanied by parallel changes at amino acids sites 10 (His to Tyr), 23 (Ile to Thr), 29 (Gly to Ala), and 82 (Ala to Phe) (supplementary table 1 and supplementary fig. 1, Supplementary Material online). The number of parallel amino acid changes between the opsin sequences was significantly greater than expected by chance ($P < 0.001$) using the test of Zhang and Kumar (1997), suggesting that they may have been under positive selection.

We used the homology model of *L. a. astyanax* L opsin from Frentiu et al. (2007) (alignment shown in supplementary fig. 3, Supplementary Material online) to investigate the position of sites inferred to change in parallel between the *A. mormo* LWRh2 sequence and *P. xuthus* PxRh3 (supplementary table 1, Supplementary Material

Table 3
Relative Rates Tests

Opsin Clades	Synonymous Sites				Nonsynonymous Sites			
	d*K*s	SD	d*K*s/SD	*P*	d*K*a	SD	d*K*a/SD	*P*
Hermeuptychia hermes LWRh1 versus *H. hermes LWRh2*[a]	0.157	0.070	2.244	0.025	0.035	0.010	3.428	0.001
Apodemia mormo LWRh1 versus *A. mormo LWRh2*[b]	0.328	0.534	0.615	0.538	0.047	0.015	3.084	0.002

NOTE.—Changes in mean synonymous (d*K*s) and nonsynonymous (d*K*a) substitution rates along with their SD.
[a] Outgroup = *Bicyclus anynana*.
[b] Outgroup = *Pieris rapae*.

online). Sites 23, 29, and 82 are located away from the retinal-binding pocket, whereas site 10 is located in the vicinity of the Schiff base. Recent work indicates that 10 amino acids modulate absorbance spectra in vertebrate violet/UV (SWS1) pigments, yet 7 of these are outside the binding pocket and act in a synergistic fashion (Wilkie et al. 2000; Yokoyama and Shi 2000; Parry et al. 2004; Yokoyama et al. 2006). It is therefore possible that substitutions at these 4 sites may be important for the evolution of these redshifted absorbance spectra.

Conclusions

Spectral shifts toward the blue in butterfly L photopigments have been shown to be the result of positive selection (Frentiu et al. 2007), although the reasons for these changes remain an open issue. In other animals, spectral changes in L visual pigments may be due to sexual selection (e.g., guppies) (Hoffmann et al. 2007) or adaptation to different light environments (e.g., Lake Victoria cichlids) (Terai et al. 2006). It is harder to establish a direct link between light environment and visual pigment spectra in terrestrial animals, as has been possible for fish (Yokoyama et al. 1999; Carleton et al. 2005), because the light environments are more complex (Endler 1993). Nonetheless, as more comparative data on visual pigment spectra and the opsin genes that encode them become available, it may be possible to link shifts in λ_{max} to particular ecological factors.

Our finding that the ancestral nymphalid, riodinid, and lycaenid photopigments appear to have had a similar λ_{max} ~540 nm allows us to speculate on the role of gene duplication in the evolution of spectral shifts. The presence of very redshifted photoreceptors in addition to green-sensitive ones in Papilionidae (575 nm and 515 nm) and Riodinidae (600 nm and 505 nm) suggests that gene duplication may permit the evolution of photoreceptors with absorbance spectrum maxima well outside the typical range of λ_{max} values achieved with only one L photoreceptor. In support of this idea, we note that in the Nymphalidae duplicated L visual pigments have not been observed in the majority of taxa and the most extreme λmax that is achieved in the long-wavelength region is 565 nm. Consequently, there appears to be an upper limit to the evolution of λmax in the long-wavelength range for butterflies with only one L photoreceptor.

Supplementary Material

Supplementary Materials and Methods, figures 1–3, and table 1 are available at *Molecular Biology and Evolution* online (http://www.mbe.oxfordjournals.org/).

Acknowledgments

We thank Lincoln Brower, Carol Boggs, Matthew Garhart, Antonia Monteiro, and John Emmel for providing specimens; Furong Yuan, Lawrence Lee, Emily N. Yee, Lisa Inouye, and Wei-Hsi Kao for technical assistance. We especially thank Steven Reppert for helpful discussions. This research was funded in part by research grants from the National Institutes of Health (EY01140 and EY00785) and National Science Foundation (NSF) (BNS-8719220) to G.D.B., NSF DEB 0640301 to A.V.Z.B., and NSF IOB-0346765 and IOS-0646060 to A.D.B.

Literature Cited

Arikawa K, Mizuno S, Kinoshita M, Stavenga DG. 2003. Coexpression of two visual pigments in a photoreceptor causes an abnormally broad spectral sensitivity in the eye of the butterfly *Papilio xuthus*. J Neurosci. 23:4527–4532.

Arikawa K, Wakakuwa M, Qiu X, Kurasawa M, Stavenga DG. 2005. Sexual dimorphism of short-wavelength photoreceptors in the small white butterfly, *Pieris rapae crucivora*. J Neurosci. 25:5935–5942.

Asenjo AB, Rim J, Oprian DD. 1994. Molecular determinants of human red/green color discrimination. Neuron. 12: 1131–1138.

Bernard GD. 1979. Red-absorbing visual pigments of butterflies. Science. 203:1125–1127.

Bernard GD. 1983a. Bleaching of rhabdoms in eyes of intact butterflies. Science. 219:69–71.

Bernard GD. 1983b. Dark-processes following photoconversion of butterfly rhodopsins. Biophys Struct Mech. 9:277–286.

Bernard GD, Douglass JK, Goldsmith TH. 1988. Far-red sensitive visual pigment of a metalmark butterfly. Invest Ophthamol. 29:350.

Bernard GD, Remington CL. 1991. Color vision in *Lycaena* butterflies: spectral tuning of receptor arrays in relation to behavioral ecology. Proc Natl Acad Sci USA. 88:2783–2787.

Briscoe AD. 1998. Molecular diversity of visual pigments in the butterfly *Papilio glaucus*. Naturwissenschaften. 85:33–35.

Briscoe AD. 2000. Six opsins from the butterfly *Papilio glaucus*: molecular phylogenetic evidence for paralogous origins of red-sensitive visual pigments in insects. J Mol Evol. 51:110–121.

Briscoe AD, Bernard GD. 2005. Eyeshine and spectral tuning of long wavelength-sensitive rhodopsins: no evidence for red-sensitive photoreceptors among five Nymphalini butterfly species. J Exp Biol. 208:687–696.

Briscoe AD, Bernard GD, Szeto AS, Nagy LM, White RH. 2003. Not all butterfly eyes are created equal: rhodopsin absorption spectra, molecular identification and localization of ultraviolet-, blue-, and green-sensitive rhodopsin-encoding mRNAs in the retina of *Vanessa cardui*. J Comp Neurol. 458:334–349.

Briscoe AD, Chittka L. 2001. The evolution of color vision in insects. Annu Rev Entomol. 46:471–510.
Britt S, Feiler R, Kirschfeld K, Zuker C. 1993. Spectral tuning of rhodopsin and metarhodopsin *in vivo*. Neuron. 11:29–39.
Brower AVZ. 1994. Rapid morphological radiation and convergence among races of the butterfly *Heliconius erato* inferred from patterns of mitochondrial DNA evolution. Proc Natl Acad Sci USA. 91:6491–6495.
Brower AVZ. 2000. Phylogenetic relationships among the Nymphalidae (Lepidoptera) inferred from partial sequences of the *wingless* gene. Proc R Soc Lond B. 267:1201–1211.
Campbell DL, Brower AVZ, Pierce NE. 2000. Molecular evolution of the *wingless* gene and its implications for the phylogenetic placement of the butterfly family Riodinidae (Lepidoptera: Papilionoidea). Mol Biol Evol. 17:684–696.
Carleton KL, Parry JWL, Bowmaker JK, Hunt DM, Seehausen O. 2005. Colour vision and speciation in Lake Victoria cichlids of the genus *Pundamilla*. Mol Ecol. 14:4341–4353.
Chan T, Lee M, Sakmar TP. 1992. Introduction of hydroxyl-bearing amino acids causes bathochromic spectral shifts in rhodopsin. Amino acid substitutions responsible for red-green color pigment spectral tuning. J Biol Chem. 267: 9478–9480.
Endler JA. 1993. The color of light in forests and its implications. Ecol Monogr. 63:1–27.
Fasick JI, Robinson PR. 1998. Mechanism of spectral tuning in the dolphin visual pigments. Biochemistry. 37:433–438.
Frentiu FD, Bernard GD, Cuevas CI, Sison-Mangus MP, Prudic KL, Briscoe AD. 2007. Adaptive evolution of color vision as seen through the eyes of butterflies. Proc Natl Acad Sci USA. 104:8634–8640.
Guindon S, Gascuel O. 2003. A simple, fast, and accurate algorithm to estimate large phylogenies by maximum likelihood. Syst Biol. 52:696–704.
Hoffmann M, Tripathi N, Henz SR, Lindholm AK, Weigel D, Breden F, Dreyer C. 2007. Opsin gene duplication and diversification in the guppy, a model for sexual selection. Proc R Soc Lond B Biol Sci. 274:33–42.
Honig B, Greenberg AD, Dinur U, Ebrey TG. 1976. Visual-pigment spectra: implications of the protonation of the retinal Schiff base. Biochemistry. 15:4593–4599.
Hsu R, Briscoe AD, Chang BSW, Pierce NE. 2001. Molecular evolution of a long wavelength opsin in mimetic *Heliconius* butterflies (Lepidoptera: Nymphalidae). Biol J Linn Soc. 72:435–449.
Kitamoto J, Sakamoto K, Ozaki K, Mishina Y, Arikawa K. 1998. Two visual pigments in a single photoreceptor cell: identification and histological localization of three mRNAs encoding visual pigment opsins in the retina of the butterfly *Papilio xuthus*. J Exp Biol. 201:1255–1261.
Kosakovsky-Pond SL, Frost SDW, Muse SV. 2005. HyPhy: hypothesis testing using phylogenies. Bioinformatics. 21: 676–679.
Lampel J, Briscoe AD, Wasserthal LT. 2005. Expression of UV-, blue-, long-wavelength-sensitive opsins and melatonin in extraretinal photoreceptors of the optic lobes of hawkmoths. Cell Tissue Res. 321:443–458.
Maddison DR, Maddison WP. 2005. MacClade: analysis of phylogeny and character evolution. Sunderland (MA): Sinauer Associates.
Maddison WP, Maddison DR. 2005. Mesquite: a modular system for evolutionary analysis.
Merbs SL, Nathans J. 1992. Absorption spectra of human cone pigments. Nature. 356:433–435.
Mullen SP. 2006. Wing pattern evolution and the origins of mimicry among North American admiral butterflies (Nymphalidae: *Limenitis*). Mol Phylogenet Evol. 39:747–758.
Okada T, Sugihara M, Bondar AN, Elstner M, Entel P, Buss V. 2004. The retinal conformation and its environment in rhodopsin in light of a new 2.2 A crystal structure. J Mol Biol. 342:571–583.
Palczewski K, Kumasaka T, Hori T, Behnke CA, Motoshima H, Fox BA, Le Trong I, Teller DC, Okada T, Stenkamp RE, et al. (12 co-authors). 2000. Crystal structure of rhodopsin: a G protein-coupled receptor. Science. 289:739–745.
Parry JWL, Poopalasundaram S, JBowmaker JK, Hunt DM. 2004. A novel amino acid substitution is responsible for spectral tuning in rodent violet-sensitive visual pigment. Biochemistry. 43:8014–8020.
Peña C, Wahlberg N, Weingartner E, Kodandaramaiah U, Nylin S, Freitas AVL, Brower AVZ. 2006. Higher level phylogeny of Satyrinae butterflies (Lepidoptera: Nymphalidae) based on DNA sequences. Mol Phylogenet Evol. 40:29–49.
Posada D, Crandall KA. 1998. Modeltest: testing the model of DNA substitution. Bioinformatics. 14:817–818.
Robinson-Rechavi M, Huchon D. 2000. RRTree: relative-rate tests between groups of sequences on a phylogenetic tree. Bioinformatics. 16:296–297.
Salcedo E, Zheng L, Phistry M, Bagg EE, Britt SG. 2003. Molecular basis for ultraviolet vision in invertebrates. J Neurosci. 23:10873–10878.
Sauman I, Briscoe AD, Zhu H, Shi DD, Froy O, Stalleicken J, Yuan Q, Casselman A, Reppert SM. 2005. Connecting the navigational clock to sun compass input in monarch butterfly brain. Neuron. 46:457–467.
Schluter D, Price T, Mooers AO, Ludwig D. 1997. Likelihood of ancestor states in adaptive radiation. Evolution. 51: 1699–1711.
Shimizu I, Yamakawa Y, Shimazaki Y, Iwasa T. 2001. Molecular cloning of *Bombyx* cerebral opsin (*Boceropsin*) and cellular localization of its expression in the silkworm brain. Biochem Biophys Res Commun. 287:27–34.
Sison-Mangus MP, Bernard GD, Lampel J, Briscoe AD. 2006. Beauty in the eye of the beholder: the two blue opsins of lycaenid butterflies and the opsin gene-driven evolution of sexually dimorphic eyes. J Exp Biol. 209:3079–3090.
Stalleicken J, Labhart T, Mouritsen H. 2006. Physiological characterization of the compound eye in monarch butterflies with focus on the dorsal rim area. J Comp Physiol. 192: 321–331.
Stavenga DG. 1975. Visual adaptation in butterflies. Nature. 254:435–437.
Stavenga DG, Arikawa K. 2006. Evolution of color and vision of butterflies. Arthropod Struct Dev. 35:307–318.
Takahashi Y, Ebrey TG. 2003. Molecular basis of spectral tuning in the newt short wavelength sensitive visual pigment. Biochemistry. 42:6025–6034.
Terai Y, Seehausen O, Sasaki T, Takahashi K, Mizoiri S, Sugawara T, Seto T, Watanabe M, Konijnendiijk N, Mrosso HDJ, et al. (14 co-authors). 2006. Divergent selection on opsins drives incipient speciation in Lake Victoria cichlids. PLoS Biol. 4:e433.
Vanhoutte KJA, Stavenga DG. 2005. Visual pigment spectra of the comma butterfly, *Polygonia c-album*, derived from in vivo epi-illumination microspectrophotometry. J Comp Physiol. 191:461–473.
Wahlberg N, Braby MF, Brower AVZ, de Jong R, Lee MM, Nylin S, Pierce NE, Sperling FAH, Vila R, Warren AD, et al. (11 co-authors). 2005. Synergistic effects of combining morphological and molecular data in resolving the phylogeny of butterflies and skippers. Proc R Soc Lond B. 272: 1577–1586.
Wahlberg N, Weingartner E, Nylin S. 2003. Towards a better understanding of the higher systematics of Nymphalidae

(Lepidoptera: Papilionoidea). Mol Phylogenet Evol. 28: 473–484.

Wakakuwa M, Stavenga DG, Kurasawa M, Arikawa K. 2004. A unique visual pigment expressed in green, red and deep-red receptors in the eye of the small white butterfly, *Pieris rapae crucivora*. J Exp Biol. 207:2803–2810.

White RH, Brown PK, Harlay AK, Bennett RR. 1983. Rhodopsing retinula cell ultrastructure and receptor potentials in the developing pupal eye of the moth *Manduca sexta*. J Comp Physiol. 150:153–163.

Wilkie SE, Robinson PR, Cronin TW, Poopalasundaram S, Bowmaker JK, Hunt DM. 2000. Spectral tuning of avian violet- and ultraviolet-sensitive visual pigments. Biochemistry. 39:7895–7901.

Yang Z. 1997. PAML: a program package for phylogenetic analysis by maximum likelihood. Comput Appl Biosci. 13: 555–556.

Yokoyama S. 2000. Molecular evolution of vertebrate visual pigments. Prog Retin Eye Res. 19:385–419.

Yokoyama S, Radlwimmer FB. 1998. The "five-sites" rule and the evolution of red and green color vision in mammals. Mol Biol Evol. 15:560–567.

Yokoyama S, Radlwimmer FB. 1999. The molecular genetics of red and green color vision in mammals. Genetics. 153: 919–932.

Yokoyama S, Shi Y. 2000. Genetics and evolution of ultraviolet vision in vertebrates. FEBS Lett. 486:167–172.

Yokoyama S, Starmer WT, Takahashi Y, Tada T. 2006. Tertiary structure and spectral tuning of UV and violet pigments in vertebrates. Gene. 365:95–103.

Yokoyama S, Zhang H, Radlwimmer FB, Blow NS. 1999. Adaptive evolution of color vision of the Comoran coelacanth (*Latimeria chalumnae*). Proc Natl Acad Sci USA. 96:6279–6284.

Zaccardi G, Kelber A, Sison-Mangus MP, Briscoe AD. 2006. Color discrimination in the red range with only one long-wavelength sensitive opsin. J Exp Biol. 209:1944–1955.

Zhang J, Kumar S. 1997. Detection of convergent and parallel evolution at the amino acid sequence level. Mol Biol Evol. 14:527–536.

Billie Swalla, Associate Editor

Accepted June 22, 2007